[2] S.-W. Chen and K . A. Zaki, "Dielectric ring resonators loaded in waveguide and on substrate," *IEEE Trans. Microwave Theory Tech.*, vol. 39, pp. 2069–2076, Dec. 1991.
[3] K. Wakino, T. Nishikawa, H. Matsumoto, and Y. Ishikawa, "Quarter wave dielectric transmission line diplexer for land mobile communications," in *IEEE MTT-S Int. Microwave Symp. Dig.*, 1979, pp. 278–280.
[4] C. L. Ren, "Mode suppressor for dielectric resonator filters," in *IEEE MTT-S Int. Microwave Symp. Dig.*, 1982, pp. 389–391.
[5] R. V. Snyder, "Dielectric resonator filters with wide stopbands," *IEEE Trans. Microwave Theory Tech.*, vol. 40, pp. 2100–2103, Nov. 1992.
[6] V. Madrangeas, M. Aubourg, P. Guillon, S. Vigneron, and B. Theron, "Analysis and realization of L-band dielectric resonator microwave filters," *IEEE Trans. Microwave Theory Tech.*, vol. 40, pp. 120–127, Jan. 1992.
[7] Y. Kobayashi and M. Minegishi, "A low-loss bandpass filter using electrically coupled high-Q $\mathrm{TM}_{01\delta}$ dielectric rod resonators," *IEEE Trans. Microwave Theory Tech.*, vol. 36, pp. 1727–1732, Dec. 1988.
[8] T. Nishikawa, K. Wakino, K. Tsunoda, and Y. Ishikawa, "Dielectric high-power bandpass filter using quarter-cut $\mathrm{TE}_{01\delta}$ image resonator for cellular base stations," *IEEE Trans. Microwave Theory Tech.*, vol. MTT-35, pp. 1150–1155, Dec. 1987.
[9] H. J. Riblet, "Waveguide filter having nonidentical sections resonant at same fundamental and different harmonic frequencies," U.S. Patent 3 153 208, 1964.
[10] K. Wakino, T. Nishikawa, H. Matsumoto, and Y. Ishikawa, "Miniaturized band pass filters using half wave dielectric resonators with improved spurious response," in *IEEE MTT-S Int. Microwave Symp. Dig.*, 1978, pp. 230–232.
[11] Y. Kobayashi and C. Inoue, "Bandpass and bandstop filters using dominant $\mathrm{TM}_{01\delta}$ mode dielectric rod resonators," in *IEEE MTT-S Int. Microwave Symp. Dig.*, 1997, pp. 793–796.
[12] R. R. Bonetti and A. E. Williams, "A narrowband filter with a wide spurious-free stopband," in *IEEE MTT-S Int. Microwave Symp. Dig.*, 1992, pp. 1331–1333.
[13] J.-F. Liang, K. A. Zaki, and A. E. Atia, "Mixed modes dielectric resonators filters," *IEEE Trans. Microwave Theory Tech.*, vol. 42, pp. 2449–2454, Dec. 1994.
[14] C. Wang, H.-W. Yao, K. A. Zaki, and R. R. Mansour, "Mixed modes cylindrical dielectric resonator filters with rectangular enclosure," *IEEE Trans. Microwave Theory Tech.*, vol. 43, pp. 2817–2823, Dec. 1995.
[15] H. Y. Hwang, N. S. Park, H. Y. Cho, S. W. Yun, and I. S. Chang, "The design of bandpass filters made of both dielectric and coaxial resonators," in *IEEE MTT-S Int. Microwave Symp. Dig.*, 1997, pp. 805–808.
[16] J.-F. Liang and W. D. Blair, "High-Q TE_{01} mode DR filters for PCS wireless base stations," *IEEE Trans. Microwave Theory Tech.*, vol. 46, pp. 2493–2500, Dec. 1998.
[17] C. Wang, K. A. Zaki, and A. E. Atia, "Dual-mode combined dielectric and conductor loaded cavity filters," in *IEEE MTT-S Int. Microwave Symp. Dig.*, 1997, pp. 1103–1106.
[18] A. Abdelmonem, J.-F. Liang, H.-W. Yao, and K. A. Zaki, "Full wave design of spurious free DR TE mode bandpass filter," *IEEE Trans. Microwave Theory Tech.*, vol. 43, pp. 744–752, Apr. 1995.
[19] R. V. Snyder and C. Alvarez, "Filters using a new type of resonator: The partially-metallized dielectric slug," in *IEEE MTT-S Int. Microwave Symp. Dig.*, 1999, pp. 1029–1032.
[20] I. C. Hunter, J. D. Rhodes, and V. Dassonville, "Dual-mode filters with conductor loaded dielectric resonators," *IEEE Trans. Microwave Theory Tech.*, vol. 47, pp. 2304–2311, Dec. 1999.
[21] H.-W. Yao, K. A. Zaki, A. E. Atia, and T. G. Dolan, "Improvement of spurious performance of combline filters," in *IEEE MTT-S Int. Microwave Symp. Dig.*, 1997, pp. 1099–1102.
[22] C. Wang, K. A. Zaki, A. E. Atia, and T. G. Dolan, "Dielectric combline resonators and filters," *IEEE Trans. Microwave Theory Tech.*, vol. 46, pp. 2501–2506, Dec. 1998.
[23] C. Wang and K. A. Zaki, "Conductor loaded resonator filters with wide spurious-free stopbands," *IEEE Trans. Microwave Theory Tech.*, vol. 45, pp. 2387–2392, Dec. 1997.
[24] A. R. Weily and A. S. Mohan, "Sandwiched conductor dielectric resonator filters for wideband spurious-free performance," in *Proc. Asia–Pacific Microwave Conf.*, 1998, pp. 1359–1362.
[25] ——, "Mode-chart calculation for dielectric- and conductor-loaded resonators using modal extraction and FDTD," *Microwave Opt. Technol. Lett.*, vol. 21, no. 6, pp. 405–411, June 1999.
[26] ——, "Full two-port analysis of coaxial probe fed TE_{01} and HE_{11} mode dielectric resonator filters using FDTD," *Microwave Opt. Technol. Lett.*, vol. 18, no. 2, pp. 149–154, June 1998.
[27] ——, "Design and wideband spurious performance prediction for a mixed resonator combline/TE_{01}-mode DR filter using FDTD," *Microwave Opt. Technol. Lett.*, vol. 23, no. 5, pp. 266–273, Dec. 1999.
[28] X.-P. Liang, K. A. Zaki, and A. E. Atia, "Dual mode coupling by square corner cut in resonators and filters," *IEEE Trans. Microwave Theory Tech.*, vol. 40, pp. 2294–2302, Dec. 1992.

Microwave Transformers, Inductors, and Transmission Lines Implemented in an Si/SiGe HBT Process

David C. Laney, Lawrence E. Larson, Paul Chan, John Malinowski, David Harame, Seshu Subbanna, Rich Volant, and Michael Case

***Abstract*—Experimental results are presented on microwave inductors, transformers, and transmission lines fabricated in an Si/SiGe heterojunction-bipolar-transistor process with standard metallization and a thick polyimide dielectric. Microstrip transmission lines with characteristic impedances from 44 to 73 Ω, Q's from 10 to 14, and insertion losses from 0.11 to 0.16 dB/mm at 10 GHz are presented. Conventional planar inductors with inductances from 0.5 to 15 nH and with peak Q's up to 22 are presented. Lateral transformers with a maximum available gain of better than -5 dB and a measured coupling coefficient (k) of 0.6 at 5.5 GHz and 0.4 up to 12.5 GHz are also discussed.**

***Index Terms*—Inductors, integrated circuit fabrication, MMICs, transformers, transmission lines.**

I. Introduction

In this paper, we present the performance of microstrip transmission lines, standard square planar inductors, and bilayer planar transformers produced with standard silicon very large scale integration (VLSI) Al–Cu metallization and a thick polyimide dielectric. In this process, the top metal (TM) layer is the standard back-end metallization, and the metal layer above the top layer, the last metal (LM) layer, is separated from the TM layer by 12 μm of polyimide (Fig. 1).

II. Silicon-Based Transmission-Line, Inductor, and Transformer Design

The design of microstrip structures, inductors, and transformers is well known in planar microwave-circuit technology. References [1]–[5], [7], and [9]–[12] provide important background.

Manuscript received April 27, 1999; revised September 22, 2000.

D. C. Laney is with the Department of Electrical and Computer Engineering, University of California at San Diego, La Jolla, CA 92093 USA and also with HRL Laboratories LLC, Malibu, CA 90265 USA.

L. E. Larson is with the Department of Electrical and Computer Engineering, University of California at San Diego, La Jolla, CA 92093 USA.

P. Chan was with Hughes Space and Communications, El Segundo, CA 90245 USA. He is now with Qualcomm Inc., San Diego, CA 92121 USA.

J. Malinowshi and D. Harame are with IBM Microelectronics, Essex Junction, VT 05452 USA.

S. Subbanna and R. Volant are with IBM Microelectronics, Hopewell Junction, NY 12533 USA.

M. Case was with HRL Laboratories LLC, Malibu, CA 90265 USA. He is now with the IBM Corporation, Encinitas, CA 92024 USA.

Publisher Item Identifier S 0018-9480(01)06142-7.

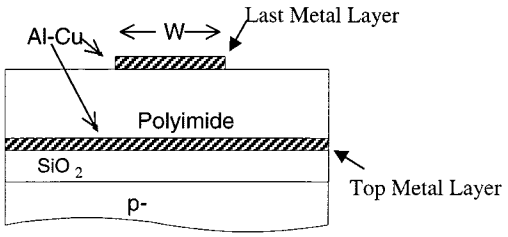

Fig. 1. Process cross section.

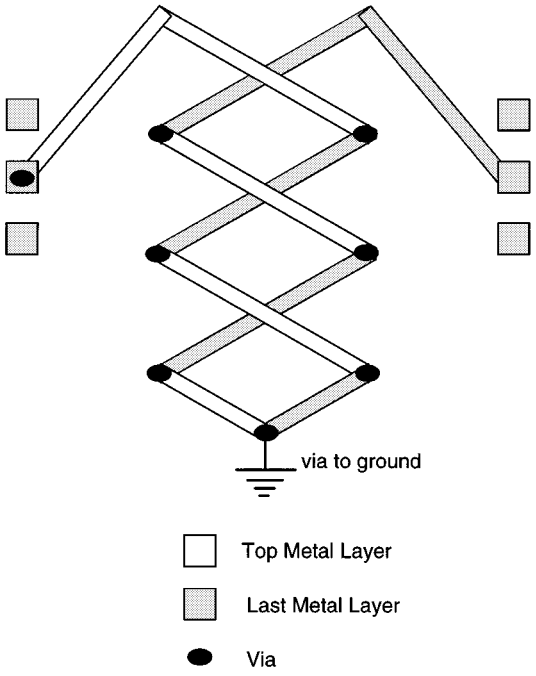

Fig. 2. Schematic top view of lateral transformer.

The lateral transformers presented here have been implemented using two metal layers in a lateral spiral design, as shown in Fig. 2. The lateral transformers were constructed so that their windings make a "flattened" coil. If one were to travel along the path of the winding from ports 1 or 2 to ground, one would see coil segments on alternating LM and TM layers.

In standard planar spiral inductors and transformers, the majority of the magnetic field is perpendicular to the substrate, causing eddy currents and ultimately loss in the substrate. Lateral devices have a magnetic field that is primarily parallel to the substrate, which should result in reduced substrate loss. On the other hand, the lateral devices have overlapping winding segments that are expected to lower the resonant frequencies compared to the standard planar devices. Lateral windings also contain many vias, increasing the series resistance. A circuit model of the transformers can be seen in Fig. 3 [13]. In this model, M is the mutual inductance, and L_1 and L_2 are the leakage inductances and do not contribute to the coupling between ports 1 and 2. Capacitors C_1 and C_3 model the capacitance between the windings and the substrate and C_2 models the interwinding capacitance. Assuming capacitors C_1, C_2, and C_3 are small, the mutual inductance M can be expressed as the imaginary part of Z_{21} divided by the angular frequency ω. The coupling coefficient is then defined as

$$k = \frac{M}{\sqrt{L_{11}L_{22}}} \tag{1}$$

where

$$L_{ii} = L_i + M \tag{2}$$

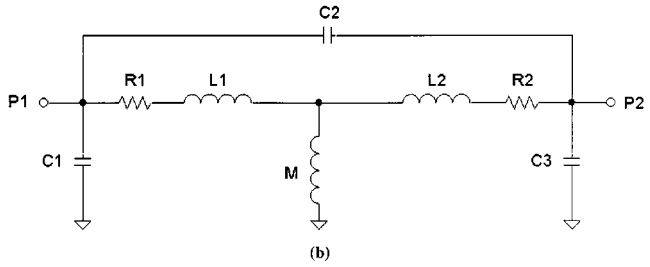

Fig. 3. Transformer equivalent-circuit model (also inductor model if M is set to zero).

L_{11} and L_{22} are the imaginary parts of Z_{11} and Z_{22}, respectively, divided by ω.

An ideal transformer has no leakage inductance and, thus, from (1) has a coupling coefficient k equal to one. In the transformer model, the leakage inductances L_1 and L_2 cause k to be less than one. Physically, the leakage inductances are due to lines of magnetic flux that link one winding, but not both.

III. Fabrication Technology

The fabrication cross section is shown in Fig. 1. The LM and TM layers consist of 2.7 μm of sputtered Al–Cu. The TM layer is separated from the substrate by approximately 3 μm of SiO_2. The dielectric is a DuPont type 5811 [6] polyimide, spun-on, and then cured to a final thickness of approximately 12 μm. Via holes are created and the resulting sidewall angle allows for excellent step coverage. This structure is similar to previously reported multichip-module (MCM) fabrication results on transmission-line structures [7], but here, the lines are fabricated directly on a silicon substrate. The conductivity of the metal is approximately 2.89×10^7 S/m. The process has been implemented on an IBM 200-mm silicon VLSI fabrication line as part of the Si/SiGe heterojunction-bipolar-transistor (HBT) BiCMOS technology [8].

IV. Experimental Results

A. Microstrip Transmission Lines

Microstrip test structures have been fabricated with various lengths, and widths of 15, 27, and 38.5 μm. The effective dielectric constant for each transmission-line width was extracted with a typical value of 2.8. Fig. 4 shows the transmission-line loss in decibels per millimeter for each width. Also shown is the calculated loss as a function of frequency for the 15-μm line using standard design equations that can be found in [5]. A polyimide loss tangent of 0.01 produced the best agreement between the measured data and predicted loss. The quality factor Q extracted for each set of transmission lines is shown in Fig. 5 and is calculated as

$$Q = \frac{\beta}{2\alpha_T} \tag{3}$$

where α_T is the real part of the extracted propagation constant and β is the imaginary part.

B. Square Planar Inductors

Planar spiral inductors on silicon substrates have been developed by several authors [9]–[11]. In our study, the square planar inductors were constructed on the LM layer. Each set consisted of a series of six inductors with an increasing number of turns.

After dembedding, the inductance and Q can be calculated from the two-port admittance parameters

$$L = \frac{1}{\omega}\mathrm{Im}\left\{\frac{1}{Y_{11}}\right\} \tag{4}$$

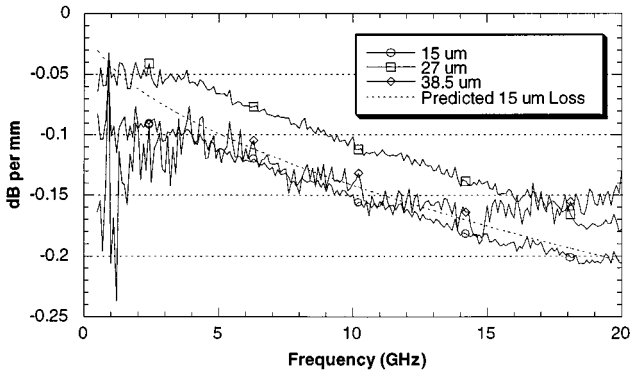

Fig. 4. Measured microstrip losses for various widths compared to calculated loss for 15-μm line.

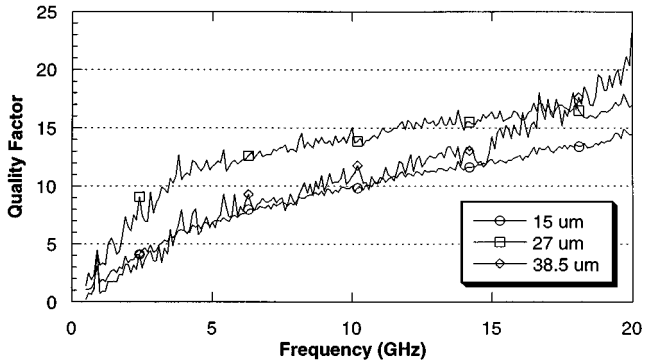

Fig. 5. Transmission-line quality factor for various widths.

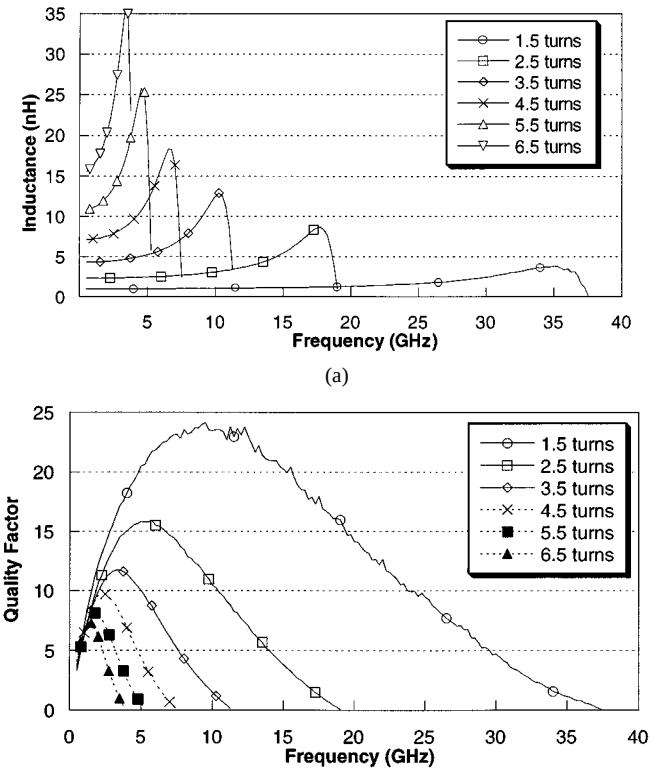

Fig. 6. Square spiral inductor. (a) Inductance. (b) Quality factor.

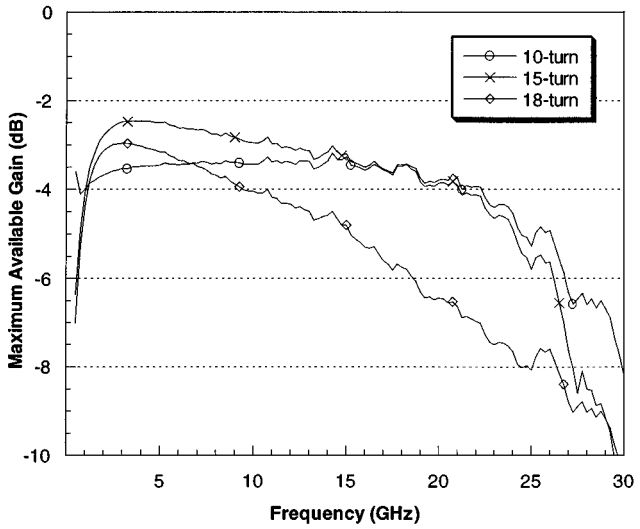

Fig. 7. Lateral transformer maximum available gain.

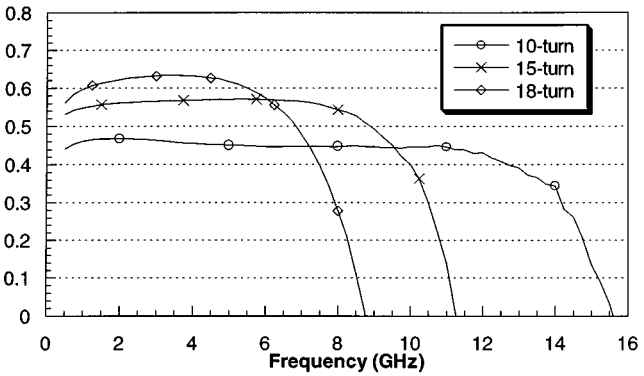

Fig. 8. Lateral transformer coupling coefficient (k).

and

$$Q = \frac{\mathrm{Im}\left\{\dfrac{1}{Y_{11}}\right\}}{\mathrm{Re}\left\{\dfrac{1}{Y_{11}}\right\}} = \frac{-\mathrm{Im}\{Y_{11}\}}{\mathrm{Re}\{Y_{11}\}}. \tag{5}$$

An equivalent circuit of the inductors is shown in Fig. 3 with $M = 0$. The peaking seen in the inductance plots is due to self-resonance. Fig. 6, the inductance and Q of the inductors, shows a peak Q of 22 at about 10 GHz.

C. Lateral Transformers

Transformers with 10, 15, and 18 turns were fabricated, each with signal conductor widths of 45 μm and winding segment lengths of 700 μm.

The loss here is greater than that presented in [3], but they have a wider bandwidth. Fig. 7 shows the maximum available gain of each transformer. It can be expressed as [14]

$$G_{ma} = \frac{1}{1-|\Gamma_{\mathrm{IN}}|^2}|S_{21}|^2\frac{1-|\Gamma_{\mathrm{OUT}}|^2}{\left|1-S_{22}\Gamma^*_{\mathrm{OUT}}\right|^2}. \tag{6}$$

The calculated parameter G_{ma} reflects the gain of the system when the source and load reflection coefficients Γ_S and Γ_L are conjugately matched to the input and output reflection coefficients of the transformer, i.e., Γ_{IN} and Γ_{OUT}, respectively. Thus, the maximum avail-

able gain occurs in (6) when $\Gamma_S = \Gamma_{\rm IN}^*$ and $\Gamma_L = \Gamma_{\rm OUT}^*$. The best gain achieved is -2.5 dB at 3 GHz with the 15-turn transformer. The useful bandwidth of the transformers can be seen from the coupling coefficients plotted in Fig. 8. The 18-turn transformer has the highest coupling coefficient (0.6), but only has usable bandwidth from 1 to 5.5 GHz. The 15-turn transformer has a lower coupling coefficient (0.5), but has a larger bandwidth from 1 to 9 GHz. The ten-turn transformer has the lowest coupling coefficient (0.4), but the largest bandwidth from 1 to 12.5 GHz. At frequencies higher than 5.5 GHz for the 18-turn transformer, 9 GHz for the 15-turn transformer, and 12.5 GHz for the ten-turn transformer, the interwinding capacitance C_2 dominates S_{21}. Above these frequencies, the structures no longer behave as transformers, but as a capacitive couplers.

V. Conclusions

Transformers, transmission lines, and inductors have been demonstrated in a production silicon VLSI HBT technology. Ten-, 15-, and 18-turn transformers have been built in a lateral orientation with wide-band performance. These devices offer improved performance from 5 to 20 GHz for silicon monolithic-microwave integrated-circuit (MMIC) applications.

Acknowledgment

The authors would like to acknowledge the support of Dr. W. Stanchina, HRL Laboratories LLC, Malibu, CA, as well as the support and encouragement of Dr. B. Meyerson, IBM Microelectronics, Essex Junction, VT, and Dr. J. Gaskill, IBM, Microelectronics, Essex Junction, VT. Author Laney would also like to thank Prof. H. J. Orchard, University of California at Los Angeles, for enlightening technical correspondence.

References

[1] M. V. Schneider, "Microstrip lines for microwave integrated circuits," *Bell Syst. Tech. J.*, vol. 48, pp. 1421–1444, May–June 1969.

[2] D. C. Laney, L. E. Larson, J. Malinowski, D. Harame, S. Subbanna, R. Volant, M. Case, and P. Chan, "Low-loss microwave transmission lines and inductors implemented in a Si/SiGe HBT process," in *IEEE Bipolar/BiCMOS Circuits Technol. Meeting*, 1998, pp. 101–104.

[3] D. Cheung, J. R. Long, R. A. Hadaway, and D. L. Harame, "Monolithic transformers for silicon RF IC design," in *IEEE Bipolar/BiCMOS Circuits Technol. Meeting*, 1998, pp. 105–108.

[4] J. R. Jams and A. Henderson, "High frequency behavior of microstrip open circuit terminations," *J. Microwaves, Opt., Acoust.*, vol. 3, no. 5, pp. 205–218, 1979.

[5] K. C. Gupta, R. Garg, and I. J. Bahl, *Microstrip Lines and Slotlines*. Norwood, MA: Artech House, 1979.

[6] DuPont, Wilmington, DE, 2611/5811 data sheet.

[7] R. G. Arnold and D. J. Pedder, "Microwave characterization of microstrip lines and spiral inductors in MCM-D technology," in *Proc. 42nd Electron. Comp. Technol. Conf.*, 1992, pp. 823–829.

[8] D. Harame *et al.*, "Si/SiGe epitaxial-base transistors—Part 1: Materials, physics and circuits," *IEEE Trans. Electron Devices*, pp. 455–468, Mar. 1995.

[9] J. N. Burghartz *et al.*, "RF components implemented in an analog SiGe bipolar technology," in *IEEE Bipolar/BiCMOS Circuits Technol. Meeting*, 1996, pp. 138–141.

[10] R. Groves, K. Stein, D. Harame, and D. Jadus, "Temperature dependence of Q in spiral inductors fabricated in a SiGe/BiCMOS technology," *IEEE Bipolar/BiCMOS Circuits Technol. Meeting*, pp. 153–156, 1996.

[11] M. Case *et al.*, "High performance microwave elements for Si/SiGe MMICs," in *IEEE Cornell Conf. Advanced Concepts High-Speed Semicond. Devices Circuits*, 1995.

[12] L. Larson *et al.*, "Si/SiGe HBT technology for low-cost monolithic microwave integrated circuits," in *Int. Solid-State Circuits Conf.*, San Francisco, CA, 1996, pp. 80–81.

[13] H. H. Skilling, *Electrical Engineering Circuits*. New York: Wiley, 1965.

[14] G. Gonzalez, *Microwave Transistor Amplifiers*. Englewood Cliffs, NJ: Prentice-Hall, 1997.